Liquid and Solid Compound Granulated Diurea Sulfate-Based Fertilizers for Sustainable Sulfur Source

J. Baltrusaitis,*,[†] A. M. Sviklas,[‡] and J. Galeckiene[‡]

[†]Department of Chemical and Biomolecular Engineering, Lehigh University, B336 Iacocca Hall, 111 Research Drive, Bethlehem, Pennsylvania 18015, United States

[‡]Department of Physical and Inorganic Chemistry, Kaunas University of Technology, Radvilenu St. 19, LT-50254 Kaunas, Lithuania

S *Supporting Information*

ABSTRACT: Design and manufacture of high nitrogen content sulfur-containing fertilizers is of crucial importance in sustainable food and energy crop production. The availability of large elemental sulfur amounts in oil refining and natural gas processing facilities, in combination with decreasing sulfur deposition into soil from natural and anthropogenic sources in a bioavailable sulfate form, calls for innovative engineering solutions that bridge this gap via sustainable sulfur processing. Diurea sulfate-based liquid and compound solid granulated fertilizers were synthesized in this work, and their resulting physicochemical properties were determined. First, phase compositional information on the $2CO(NH_2)_2 \cdot H_2SO_4 - CO(NH_2)_2 - H_2O$ ternary system was measured, and high nitrogen content, ~15:1 N:S ratio liquid fertilizer grades, were established. Next, diurea sulfate granulation experiments using (i) dolomite, (ii) byproduct material after the phosphoric acid extractive production, $CaSO_4 \cdot 0.5H_2O$, and (iii) dolomite combined with diammonium phosphate, $(NH_4)_2HPO_4$, and potassium chloride, KCl, were performed. Using diurea sulfate, 16−16−16−5.5(S)−0.4(MgO)−0.6(CaO) compound granulated fertilizers were successfully obtained, and time-resolved changes in their crystalline phase composition during granule curing were monitored using XRD. The granule crushing strength measured increased to 3.800 MPa within the 30 day storage thus resulting in high quality fertilizer material.

KEYWORDS: *Diurea sulfate, Polytherm, Phase composition, Compound granulated fertilizer*
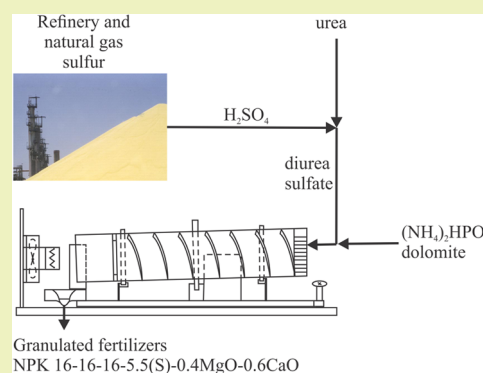
INTRODUCTION

The ever-increasing World population and urbanization does not allow for a continuous increase in arable land area necessary to increase the cultivation of crops, which is so vital for humanity's existence. Global demand for food is projected to increase by 40% by 2030, but the land currently used for agriculture is already close to the sustainable limit of 15% of the Earth's surface that can be exploited for crop production.[1,2] Additionally, rapid global warming, due to the depletion of the nonrenewable hydrocarbon feedstock and the concurrent greenhouse gas emissions, are driving an increase in the production and use of the alternative, CO_2 neutral, transportation fuels and chemicals obtained from the biomass grown on both fertile and marginal land.[3] Due to these reasons, crop yields per unit area need to be continuously increased. Proper nutrition of crops using major nutrients (e.g., N, P, K, Ca, Mg, and S) is thus mandatory because the most important constraints to crop growth are due to a deficiency of these nutrients in soil. Sulfur is a secondary plant nutrient that is essential for healthy growth and development of plants. It is an integral part of plant amino acids and proteins and plays an important role in their redox control of cellular processes.[4] For example, winter oilseed rape (*Brassica napus* L.), a plant of major agro-economic importance with yields of 47 million tons

worldwide in 2007 and with wide use in the production of oil and sustainable fuels, has reduced yields up to 40% without adequate supply of S.[5] This is because at the cellular level sulfur deficiency leads to a particularly strong decrease in nitrate reductase activity and consecutively in a reduced nitrate uptake relative to ammonium.[6] It has been well established that sulfur deficiency can strongly reduce nitrogen use efficiency (ratio of harvested nitrogen to nitrogen fertilization).[5,7] Thus, for the plants to efficiently uptake and metabolize the major nutrient nitrogen, a sufficient amount of sulfur must be present. While the required N:S ratio varies for different crops, a value of 15:1 can be taken as optimal in most cases.[8]

In recent years, a clear sulfur deficiency in soil has been observed globally and forecasted to increase.[9−12] This is due to several reasons. First, dimethyl sulfide (DMS), a byproduct of phytoplankton production, was recently detected at significantly lower concentrations in seawater with low pH, resulting from anthropogenic carbon dioxide uptake by the oceans.[13] Oceanic DMS emissions constitute the largest natural source of atmospheric sulfur[14] because DMS is emitted into the

atmosphere where its oxidation products include gas-phase sulfuric acid.[15] Global DMS emissions are projected to decrease by about 18% in 2100 compared with preindustrial times due to the combined effects of ocean acidification and climate change.[16] Second, new fertilizers that lack sulfur are increasingly being used. They are routinely prepared nowadays using sulfur-free inorganic acids, such as HNO_3 or H_3PO_4. Finally, anthropogenic emissions of sulfur compounds due to fuel combustion in internal combustion engines are projected to decrease.[17] This is due to the stringent regulations put forth by governments worldwide which in turn require ultradeep (<1 ppmw) removal of sulfur from transportation fuels.[18,19] Thus, there is a pressing need to design fertilizers that would incorporate sulfur into the soil.

The World sulfur production, on the other hand, is increasing. It is primarily due to increased sulfur concentration in crude oil and sour natural gas because low sulfur hydrocarbon fuel reserves are dwindling. Sulfur is detrimental in the refining process as it tends to deactivate certain catalysts used in crude oil processing and causes corrosion problems in pipelines, pumping, and refining equipment. Thus, it is removed via catalytic a hydrodesulfurization process to form H_2S, which is then converted to form elemental sulfur.[20] Currently, about 60 million tons of elemental sulfur is generated in refineries annually and stored in the form of powder due to the rather small elemental sulfur demand.[21] This provides an excellent opportunity to combine this excess sulfur with nitrogen-based fertilizers for sustainable crop production. Plants take up sulfur from the soil primarily in the form of sulfate,[22] while refineries generate sulfur in its elemental form.[21] There are, however, well-established large-scale technologies to convert elemental sulfur to sulfuric acid, H_2SO_4. In fact, the majority of the elemental sulfur currently consumed is converted into H_2SO_4, which is also later used in phosphate fertilizer production. A major fertilizer currently used that contains both nitrogen and sulfur is ammonium sulfate, $(NH_4)_2SO_4$, with 21−0−0−24(S) nutrient (N−P−K−S) composition. This is mostly due to its availability from caprolactam production[23] or a flue gas desulfurization by-product.[24] Other liquid sulfur-containing nitrogen fertilizers are currently mostly based on ammonium thiosulfate (12−0−0−26(S)). These fertilizers have rather low nitrogen content and/or an unbalanced N−S ratio. Thus, of major interest is obtaining N−S fertilizers with large nitrogen content utilizing elemental sulfur via a sulfuric acid proxy.

Urea has the largest N-content in granular fertilizers (46%). It has also been known to react with acids, including H_2SO_4.[25] Solid urea−ammonium sulfate with several high nitrogen content compositions, such as 40−0−0−4(S) and 30−0−0−13(S), has previously been granulated from concentrated (>99%) urea melt and crystalline $(NH_4)_2SO_4$.[26] Diurea sulfate (2:1) has a rather high nitrogen content (26−0−0−15(S)) and has been isolated previously in its solid form.[27] A series of patents from the 1980s were filed and granted by Union Oil Company of California,[28−33] utilizing fundamental knowledge, obtained from the early work of Lawrence H. Dalman, who investigated crystalline phases present in a ternary $CO(NH_2)$−H_2SO_4−H_2O system.[25] They claimed they could synthesize solutions of mono- and diurea sulfate with rather high sulfur content. The problem that has not been addressed to date calls for the fundamental understanding and new engineering concepts in synthesizing N−S containing fertilizers, while delivering the most efficient fertilizers with N:S ratios of 15:1

that also have the largest possible nitrogen concentration. For this purpose, we investigated and devised a phase diagram of a high nitrogen content material, diurea sulfate, in phase equilibrium with urea and H_2O, thus obtaining a high nitrogen content. We then synthesized liquid diurea sulfate-based fertilizers using diurea sulfate, urea. and aqueous H_2SO_4 and explored their resulting compositional and crystalline phase landscapes in order to establish the concentration and temperature boundaries suitable for stable liquid fertilizers. Finally, we performed granulation of the compound granulated N−P−K fertilizers using diurea sulfate as a high nitrogen content sulfur-containing material and explored their structural and chemical properties.

■ EXPERIMENTAL DETAILS

$2CO(NH_2)_2 \cdot H_2SO_4$ Synthesis. Diurea sulfate (2:1 molecular ratio of urea to H_2SO_4) was synthesized using the corresponding stoichiometric ratios of the reactants. Chemicals used—urea ($CO(NH_2)_2$) and sulfuric acid (H_2SO_4) (95−98%)—were obtained from Aldrich and were ACS reagent grade. Distilled water was used as a solvent where necessary. Synthesis was performed by carefully dosing H_2SO_4 under vigorous stirring while cooling the reaction vessel. Solid urea has a melting point of 133 °C, and with slow heating, it begins decomposing at ∼80 °C.[34] For this reason, the synthesis temperature was maintained below 60 °C at all times. Typical H_2SO_4 dosing took 5−7 min, after which the resulting solution was left to settle down. Crystals were obtained within 1−2 weeks and dried over concentrated H_2SO_4 until a constant sample mass. Calculated synthesis yield was 99.1%. Elemental analysis of the solid material obtained showed 25.50% (wt) (vs 25.7% theoretical) urea nitrogen, 14.6% (wt) sulfur (vs 14.7% theoretical), and no ammoniacal nitrogen, thus confirming pure diurea sulfate and no urea hydrolysis. Finally, XRD analysis of the crystalline $2CO(NH_2)_2 \cdot H_2SO_4$ material yielded a diffraction pattern with the corresponding peaks, analogous as those reported in the literature for $2CO(NH_2)_2 \cdot H_2SO_4$.[27]

Solubility Experiments. Solubility measurements of binary $2CO(NH_2)_2 \cdot H_2SO_4$−$H_2O$ and ternary $2CO(NH_2)_2 \cdot H_2SO_4$−$CO(NH_2)$−$H_2O$ mixtures were determined using a visual polythermal method. The liquidus temperature is the temperature at which the first crystals appear during cooling and the last crystal disappears during heating. The average value is then taken as the liquidus temperature. Typical cooling agents used were chosen depending on the crystallization temperature of the solids and were as follows: (i) ice + KCl (cooling to −11.0 °C), (ii) ice + NH_4NO_3 (cooling to −17.3 °C), (iii) ice + NaCl (cooling to −21.2 °C), and (iv) dry ice + ethanol (cooling to −72.0 °C).

For the solubility measurements, 5 g of the solution was used, and temperature was measured using a Hg thermometer with the standard error of ±0.1 °C.

Chemical Analysis. Total nitrogen and urea nitrogen were determined using Kjeldahl digestion. Briefly, urea is transformed quantitatively into ammonia by boiling in the presence of sulfuric acid. The ammonia thus obtained is distilled from an alkaline medium, the distillate being collected in an excess of standard sulfuric acid. The excess acid is titrated by means of a standard alkaline solution.[35]

Instrumental Analysis. XRD analysis was performed using a DRON-6 instrument equipped with a Cu anode (λ = 0.154 nm). Diffraction patterns were acquired for 2Θ angles from 4° to 70°. For identification of the compounds, the International Center for Diffraction Data (ICDD) PDF-2 database was used. Diurea sulfate, $2CO(NH_2)_2 \cdot H_2SO_4$, a reference compound, was not present in ICDD PDF-2. Thus, the d-values of the synthesized diurea sulfate, obtained from the XRD data of the crystallized material, were compared against those extracted from the diurea sulfate crystalline data obtained by Chen et al.[27] For this purpose, literature unit cell data was read into Mercury,[36] and the diurea sulfate XRD spectrum was simulated. 2Θ values of the simulated peaks were converted into d-values using

Bragg's law. These were used for identification of the XRD peaks obtained from the diurea sulfate synthesized in this work.

Differential thermal analysis was performed using a Du Pont Instruments 990 thermal analyzer operating at 10 mV/cm sensitivity and 10 °C/min temperature ramp time. Aluminum oxide was used as the inert material.

Crushing strength is a measure of the granule resistance to deformation or fracture under pressure. It is a crucial parameter in estimating the expected handling and storage properties of the granular material obtained. Granule crushing strength was determined by applying a constant force until the granule lost its structural integrity, according to the modified procedure IFDC S-115.[37] In particular, 25 granules were analyzed, highest and lowest values were not accounted for, and an averaged crushing strength value was obtained. The equipment consists of an automated press controlled by a stepping motor that can apply a force from 5 to 200 N. The measured granule diameter (2 to 4 mm) was then used to obtain the final crushing strength values in units of MPa. No standard deviation is typically reported, according to the procedure.

Compound $2CO(NH_2)_2 \cdot H_2SO_4$-Based Fertilizer Granulation. Technical grade H_2SO_4 (94%) and 18−46−0 technical diammonium phosphate from SC "Lifosa" (Kedainiai, Lithuania), technical grade urea (46.3% N) from SC "Achema" (Jonava, Lithuania), and technical grade KCl (60−62% K_2O) from JSC "Belaruskali" (Belarus) were used in compound N−P−K fertilizer granulation experiments. Urea was obtained prilled in the form of 2−4 mm granules and was milled and sieved to obtain <0.5 mm particles prior to granulation.

Other raw materials investigated to be granulated with diurea sulfate were as follows. Dolomite ($CaCO_3 \cdot MgCO_3$) powder obtained from an industrial dolomite extraction and processing site (Petrasiunai, Lithuania) with a particle size of <0.5 mm and elemental composition, in weight %, of 28.81 CaO, 19.98 MgO, 1.71 Fe_2O_3, 0.10 Al_2O_3, 2.10 SiO_2, 1.76×10^{-2} Mn, 2.71×10^{-2} Zn, 1.54×10^{-3} Cr, 3.34×10^{-4} Cu, 2.81×10^{-4} Ni, 8.51×10^{-4} Co, 2.50×10^{-4} Mo, 9.79×10^{-5} Cd, 4.69×10^{-6} Pb, $< 1 \times 10^{-6}$ Se, and $<1 \times 10^{-6}$ Hg was used as a filler material. Calcium hemihydrate−phosphogypsum ($CaSO_4 \cdot 0.5H_2O$) was obtained from SC "Lifosa" (Kedainiai, Lithuania) as the phosphoric acid manufacturing byproduct and contained, in weight %, 32.74 CaO, 52.04 SO_3, 1.33 P_2O_5, 0.23 F, 15.71 moisture, and 0.99 of insoluble material.

Solid compound fertilizer granules were obtained using a lab scale rotary drum granulator dryer with a length (L) of 0.45 m and a diameter (D) of 0.11 m (Figure 6). The L/D ratio was thus 4.09, similar to those typically used in granulated phosphorus fertilizer manufacturing, to maintain similar granule residence time in the drum. The granulator inclination angle was varied from 2° to 5°, whereas its rotation speed was 20 min^{-1}, similar to those used for NPK fertilizer granulation.[38] The granulator was manufactured using polyvinyl chloride and was equipped with a counterflow forced air electric heater to ensure crystalline water formation and consecutive product drying. Typically, the air temperature entering the granulator was fixed at 35 °C. A slurry of N−P−K component particles of <0.5 mm, together with the necessary amount of moisture in the form of water, was prepared and thoroughly mixed prior to granulation and then supplied into the granulator drum. Collected granules were sieved using metal wire cloth sieves from Retsch (DIN-ISO 3310-1), and the size fraction between 2 and 4 mm was collected. Is chemical, as well as structural properties, were analyzed.

■ RESULTS AND DISCUSSION

$2CO(NH_2)_2 \cdot H_2SO_4$−$H_2O$ Binary System Phase Composition. It has long been known that urea exothermally reacts with inorganic acids making stable complexes.[25] Diurea sulfate, however, has only been relatively recently isolated in its crystalline form and confirmed crystalographically.[27] Diurea sulfate, from the standpoint of making nitrogen- and sulfur-containing fertilizers, is advantageous over urea sulfate because it contains more nitrogen per molecular unit. Because its

solubility in water is different from that of a well-known urea in solution, we constructed a binary $2CO(NH_2)_2 \cdot H_2SO_4$−$H_2O$ phase diagram using a polythermal method with the results shown in Figure 1. First, it is shown that diurea sulfate dissolves

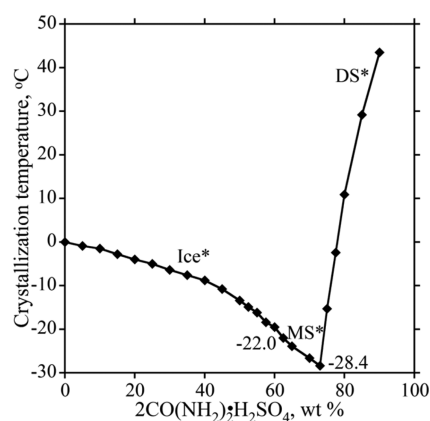**Figure 1.** Measured polytherm of $2CO(NH_2)_2 \cdot H_2SO_4$ dissolution in H_2O. Three different solid phases were detected, namely Ice* (ice), MS* (monourea sulfate), and DS* (diurea sulfate). Two critical points were found at −22.0 and −28.4 °C.

well in water. At 40 °C, a mixture containing 88.5% of diurea sulfate can be made. Second, the $2CO(NH_2)_2 \cdot H_2SO_4$−$H_2O$ binary system crystallization curve is comprised of three regions, where either ice (Ice*), (mono)urea sulfate (MS*), and diurea sulfate (DS*) crystallize out of the saturated solution. The first critical point is detected at −22.0 °C with the corresponding solution composition of 62.5% $2CO(NH_2)_2 \cdot H_2SO_4$ and 37.5% H_2O. The solid phase at this critical point was analyzed, and both ice and urea sulfate were detected. When the $2CO(NH_2)_2 \cdot H_2SO_4$ concentration reaches 73% in this binary system at −28.4 °C, the second critical—eutectic—point is detected. Measured crystalline material obtained at this point was comprised only from $CO(NH_2)_2 \cdot H_2SO_4$ and $2CO(NH_2)_2 \cdot H_2SO_4$. By further increasing the $2CO(NH_2)_2 \cdot H_2SO_4$ amount in the binary mixture, the crystallization temperature sharply rises with the only solid phase crystallized and confirmed as being $2CO(NH_2)_2 \cdot H_2SO_4$. A very important observation can be made that diurea sulfate can be recrystallized from its aqueous solutions without losing its crystalline form or stoichiometric composition, for example, not forming monourea sulfate with the corresponding undesired loss of its high nitrogen content.

$2CO(NH_2)_2 \cdot H_2SO_4$−$CO(NH_2)_2$−$H_2O$ Ternary System Phase Composition. It is known that the optimal N:S ratio of 15:1 needs to be achieved for an efficient uptake of nitrogen.[8] In $2CO(NH_2)_2 \cdot H_2SO_4$, this ratio is 1.75. Thus, additional urea needs to be added in an attempt to attain this high nutrient ratio. Because nutrient composition depends on the solubility of the corresponding molecular components in water, crystallization temperatures in saturated aqueous solutions must be determined. For this purpose, the $2CO(NH_2)_2 \cdot H_2SO_4$−$CO(NH_2)_2$−$H_2O$ ternary phase composition was explored, and a phase diagram was constructed based on the compositions, as shown in Table 1. In particular, a series of fixed ratio $2CO(NH_2)_2 \cdot H_2SO_4$−$H_2O$ solutions from I through VIII were prepared, and the amount of $CO(NH_2)_2$ added was varied. Further, a series of fixed ratio $CO(NH_2)_2$−H_2O solutions from IX through XIII were prepared, and the amount

Table 1. $2CO(NH_2)_2 \cdot H_2SO_4 - CO(NH_2)_2 - H_2O$ Ternary Phase Composition Used in Analysis[a]

number	mass composition
I	$(5 - x)[10\%\ 2CO(NH_2)_2 \cdot H_2SO_4 + 90\%\ H_2O] + xCO(NH_2)_2$
II	$(5 - x)[20\%\ 2CO(NH_2)_2 \cdot H_2SO_4 + 80\%\ H_2O] + xCO(NH_2)_2$
III	$(5 - x)[30\%\ 2CO(NH_2)_2 \cdot H_2SO_4 + 70\%\ H_2O] + xCO(NH_2)_2$
IV	$(5 - x)[40\%\ 2CO(NH_2)_2 \cdot H_2SO_4 + 60\%\ H_2O] + xCO(NH_2)_2$
V	$(5 - x)[50\%\ 2CO(NH_2)_2 \cdot H_2SO_4 + 50\%\ H_2O] + xCO(NH_2)_2$
VI	$(5 - x)[60\%\ 2CO(NH_2)_2 \cdot H_2SO_4 + 40\%\ H_2O] + xCO(NH_2)_2$
VII	$(5 - x)[70\%\ 2CO(NH_2)_2 \cdot H_2SO_4 + 30\%\ H_2O] + xCO(NH_2)_2$
VIII	$(5 - x)[80\%\ 2CO(NH_2)_2 \cdot H_2SO_4 + 20\%\ H_2O] + xCO(NH_2)_2$
IX	$(5 - x)[10\%\ CO(NH_2)_2 + 90\%\ H_2O] + x[2CO(NH_2)_2 \cdot H_2SO_4]$
X	$(5 - x)[20\%\ CO(NH_2)_2 + 80\%\ H_2O] + x[2CO(NH_2)_2 \cdot H_2SO_4]$
XI	$(5 - x)[30\%\ CO(NH_2)_2 + 70\%\ H_2O] + x[2CO(NH_2)_2 \cdot H_2SO_4]$
XII	$(5 - x)[40\%\ CO(NH_2)_2 + 60\%\ H_2O] + x[2CO(NH_2)_2 \cdot H_2SO_4]$
XIII	$(5 - x)[50\%\ CO(NH_2)_2 + 50\%\ H_2O] + x[2CO(NH_2)_2 \cdot H_2SO_4]$

[a]Total of 5 g of material was used, and x varied from 0 to 5.

of $2CO(NH_2)_2 \cdot H_2SO_4$ added was varied. The corresponding polytherms were measured in the temperature range up to 40 °C, and the data obtained are shown in Figures 2 and 3, respectively. From Figure 2, it is observed that the crystallization curves for the I through VI solution compositions are comprised of two main components in the solid phase: ice and $CO(NH_2)_2$. With an increase in $CO(NH_2)_2$ concentration but before the eutectic point, crystallization temperature decreases and ice crystallizes from the saturated

solution, whereas after the eutectic point, the crystallization temperature starts to increase and urea is the solid crystallized product. The crystallization curve corresponding to the VII composition solution exhibits a similar behavior to those of I through VI. However, monourea sulfate crystallizes before the eutectic point. Analogously, the VIII composition solution has diurea sulfate crystallizing before the eutectic point.

Composition solutions IX through XIII have crystallization curves of fixed $CO(NH_2)_2$ to H_2O ratios but vary as a function of $2CO(NH_2)_2 \cdot H_2SO_4$ concentration, shown in Figure 3. It is shown that IX through XI curves are comprised of three regions: ice, $CO(NH_2)_2$, and $2CO(NH_2)_2 \cdot H_2SO_4$. Every curve has two critical points due to the phase changes that occur. Crystallization curve XII is comprised of four different regions due to $CO(NH_2)_2$, ice, monourea sulfate, and diurea sulfate. Importantly, when diurea sulfate is added to the saturated urea solution, urea crystallization temperature decreases until the critical point at −16.5 °C, which has the composition of 30% urea, 25% diurea sulfate, and 45% water. The solid phase detected at this critical point was comprised of both urea and ice. Further increase in the diurea sulfate amount further decreases the crystallization temperature with the solid ice phase detected. The second critical point was detected at −26.4 °C with the corresponding solid phase due to both ice and monourea sulfate. A third critical (eutectic) point was detected at −39.2 °C with the corresponding solution composition of 15% urea, 62.5% diurea sulfate, and 22.5% H_2O. The solid phase is comprised of both monourea and diurea sulfates. After
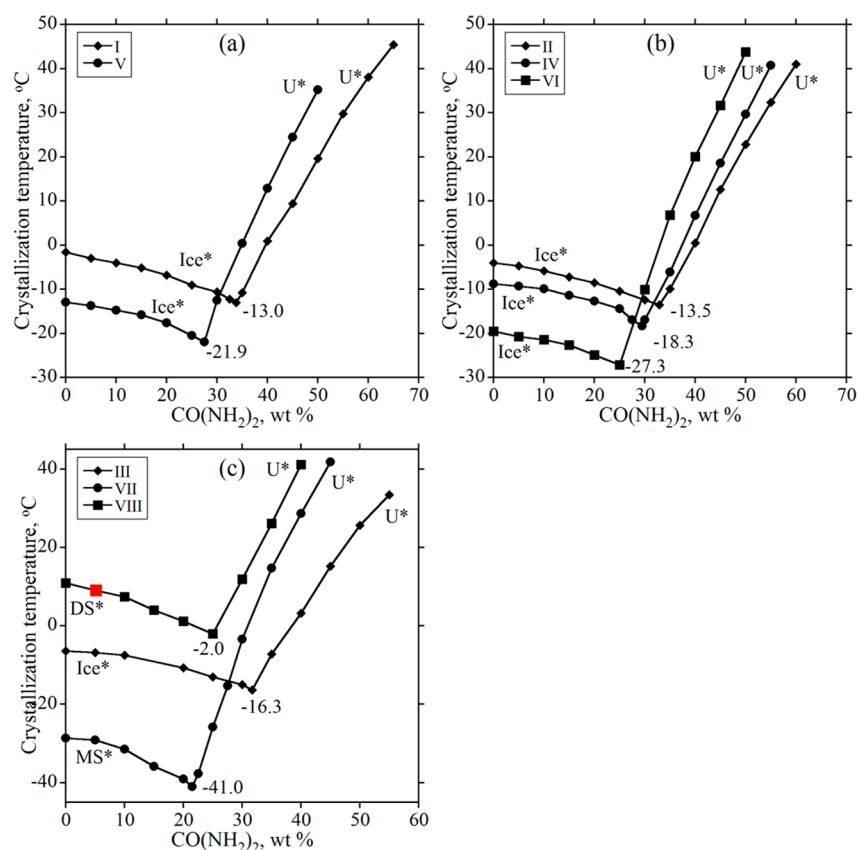
Figure 2. Measured polytherms of ternary $2CO(NH_2)_2 \cdot H_2SO_4 - CO(NH_2)_2 - H_2O$ varying composition system crystallization for (a) I and V, (b) II, IV, and VI, and (c) III, VII, and VIII solution compositions, shown in Table 1. A fixed mass ratio of $2CO(NH_2)_2 \cdot H_2SO_4$ to H_2O was used at each data point, and $CO(NH_2)_2$ was added to obtain the total analyte mass of 5 g. Red squares show representative solution compositions analyzed with differential thermal analysis, shown in Figure 4.
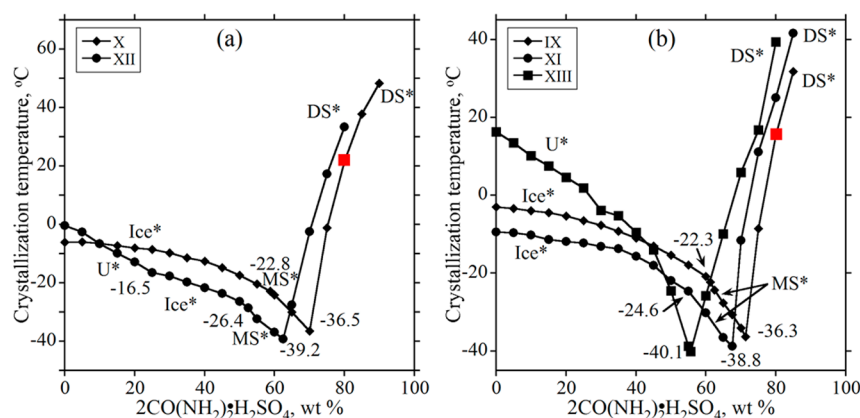
Figure 3. Measured polytherms of ternary $2CO(NH_2)_2 \cdot H_2SO_4 - CO(NH_2)_2 - H_2O$ varying composition system crystallization for (a) X and XII, (b) IX, XI and XIII solution compositions, shown in Table 1. Fixed mass ratio of $CO(NH_2)_2$ to H_2O was taken at each data point and $2CO(NH_2)_2 \cdot H_2SO_4$ was added to obtain total analyte mass of 5 g. Red squares show representative solution compositions analyzed with differential thermal analysis shown in Figure 4

Table 2. $2CO(NH_2)_2 \cdot H_2SO_4 - CO(NH_2)_2 - H_2O$ Critical Points with the Corresponding Solution and Solid Phase Compositions

sample	solution composition (wt %)			crystallization temperature (°C)	solid phase detected
	$CO(NH_2)_2$	$2CO(NH_2)_2 \cdot H_2SO_4$	H_2O		
I	33.80	6.62	59.58	−13.0	Ice*+U*
II	32.90	13.42	53.68	−13.5	Ice*+U*
III	31.70	20.49	47.81	−16.3	Ice*+U*
IV	29.50	28.20	42.30	−18.3	Ice*+U*
V	27.50	36.25	36.25	−21.9	Ice*+U*
VI	25.00	45.00	30.00	−27.1	Ice*+MS*+U*
VII	21.50	54.95	23.55	−41.0	MS*+DS*+U*
VIII	25.00	60.00	15.00	−2.0	DS*+U*
IX	3.87	61.30	34.83	−22.3	Ice*+MS*
	2.87	71.30	25.83	−36.3	MS*+DS*
X	8.24	58.80	32.96	−22.8	Ice*+MS*
	6.00	70.00	24.00	−36.5	MS*+DS*
XI	13.50	55.00	31.50	−24.6	Ice*+MS*
	9.75	67.50	22.75	−38.8	MS*+DS*
XII	30.00	25.00	45.00	−16.5	Ice*+U*
	20.00	50.00	30.00	−26.4	Ice*+MS*
	15.00	62.50	22.50	−39.2	MS*+DS*
XIII	22.15	55.70	22.15	−40.1	DS*+U*

the third critical point, the crystallization temperature starts increasing, and the only solid phase crystallized is due to the diurea sulfate. Finally, the XIII composition solution crystallization curve is comprised of two solid components. Before the eutectic point, urea crystallizes from the saturated solution, whereas afterward, diurea sulfate is the crystallized compound. The eutectic point is detected at −40.1 °C at a solution composition of 22.15% urea, 55.7% diurea sulfate, and 22.14% water. The solid phase crystallized at the eutectic point is due to both urea and diurea sulfate. The critical point data measured, along with the corresponding solution phase and crystallized solid phase composition, are summarized in Table 2. It is shown that within the concentration ranges analyzed, low (<0 °C) crystallization temperatures are detected that vary between −2.0 and −41.0 °C. Solid phases detected were ice, urea, and mono- and diurea sulfates. The absolute lowest temperature of −41.0 °C had a solution composition of 21.50% urea, 54.95% diurea sulfate, and 23.55% water.

The information obtained from the polytherms shown in Figures 3 and 4 was used to construct a ternary $2CO(NH_2)_2 \cdot$ $H_2SO_4 - CO(NH_2)_2 - H_2O$ system diagram shown in Figure 5. Solubility of the binary urea−H_2O system has previously been determined in the literature using DSC experiments and X-ray scattering measurements.[39] The compound at the eutectic point was determined to be a mixture of two crystalline materials: urea and ice. Its melting temperature was determined to be −12.5 °C, and it contained 29.4% of urea. This point is included in Figure 5, as well as the two points of the binary $2CO(NH_2)_2 \cdot H_2SO_4 - H_2O$ system with 62.5% and 73.0% $2CO(NH_2)_2 \cdot H_2SO_4$ corresponding to −22.0 and −28.4 °C crystallization temperatures. The $2CO(NH_2)_2 \cdot H_2SO_4 - CO-(NH_2)_2 - H_2O$ system shown is comprised of four crystallization regions—ice, urea, and mono- and diurea sulfate—separated by a black polytherm lines. From this ternary diagram it can be seen, that the presence of urea in the solution decreases the solubility of diurea sulfate. On the other hand, addition of the diurea sulfate to the solution increases the solubility of urea.

Elemental and Thermogravimetric Analysis of Solid Samples Crystallized from $2CO(NH_2)_2 \cdot H_2SO_4 - CO(NH_2)_2 - H_2O$ Ternary System. Solid phase material, crystallized out of
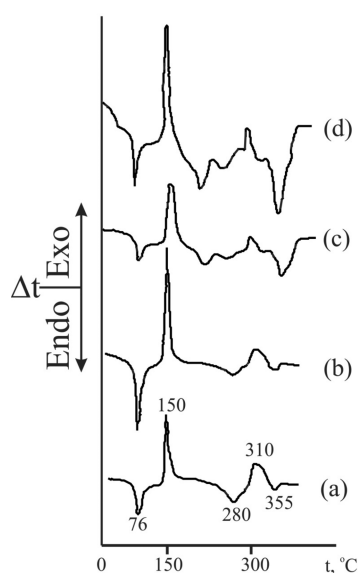
Figure 4. Differential thermal analysis (DTA) curves of (a) as-synthesized diurea sulfate and the representative solid phase material crystallized out of (b) 5.0% U* + 76.0% DS* + 19.0% H₂O, (c) 2.0% U* + 80.0% DS* + 18.0% H₂O, and (d) 4.0% U* + 80.0% DS* + 16.0% H₂O solution compositions. Curve (b) is from Figure 2 curve VIII. Curve (c) is from Figure 3 curve IX. Curve (d) is from Figure 3 curve X. These points are shown in Figures 2 and 3 by the red circles.
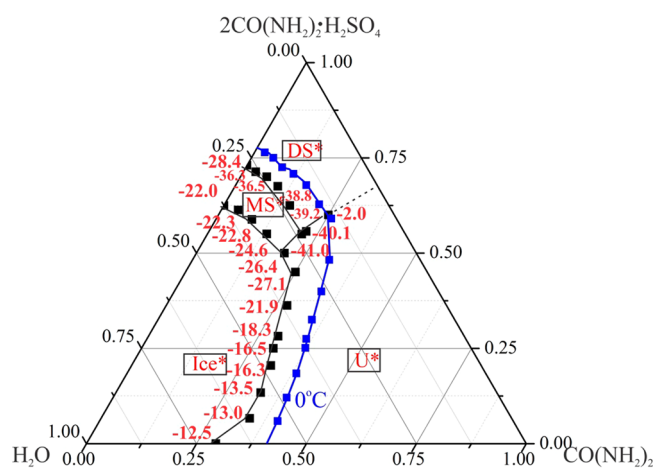

Figure 5. Measured phase diagram of the ternary $2CO(NH_2)_2 \cdot H_2SO_4 - CO(NH_2)_2 - H_2O$ system. Four distinct crystalline phase regions—Ice* (ice), U* (urea), MS* (monourea sulfate), and DS* (diurea sulfate)—can be distinguished by the black polytherm curve connecting the eutectic points measured. Crystallization temperatures are shown in red next to the corresponding points. The saturated solution crystallization isotherm at 0 °C corresponding to that of liquid fertilizer is shown in blue. Lines are for eye guidance only. Concentrations are expressed in terms of fraction for brevity.

the saturated solutions of the polytherm curves shown in Figures 2 and 3, was analyzed to obtain their elemental composition and thermal and crystalline phase information. This was done in order to establish the identity of the solid phase that is critical for creating liquid fertilizers of high nitrogen content. Of particular importance was to obtain the saturated solution compositions where diurea sulfate, DS*, crystallizes. First, to verify the material, XRD patterns were obtained for the DS* material crystallized and showed peaks with the corresponding interplanar spacing of 0.779, 0.665,

0.581, 0.571, 0.541, 0.530, 0.504, 0.480, 0.393, 0.378, 0.352, 0.330, 0.324, 0.314, 0.286, 0.258, and 0.160 nm. These values agree very well with those obtained using the experimentally reported diurea sulfate crystal structure.[27] Next, thermogravimetric analyses of pure DS* and solid phase crystallized out of 5.0% U* + 76.0% DS* + 19.0% H₂O, 2.0% U* + 80.0% DS* + 18.0% H₂O, and 4.0% U* + 80.0% DS* + 16.0% H₂O solution compositions was performed and are shown in Figure 4. To the authors' knowledge, there is no literature data discussing diurea sulfate thermal transitions. Hence, thermal transition assignments were made by adapting urea thermal analysis data and reevaluating it by accounting for the H₂SO₄ molecule availability, for example, in an acidic environment. First, an endothermal transition starting at 76 °C due to the melting of DS* is observed, as well as the second starting at 150 °C due to the decomposition of DS*. Thermal transitions at higher temperatures of 280, 310, and 355 °C are due to the complex higher order urea decomposition reactions.[40−42] Most importantly, solid DS* phases crystallized out of various compositions of the ternary $2CO(NH_2)_2 \cdot H_2SO_4 - CO(NH_2)_2 - H_2O$ system, and as shown in Figure 4b, c, and d, exhibited the same thermal effects as those of the pure $2CO(NH_2)_2 \cdot H_2SO_4$ shown in Figure 4a. No peak was observed at 100 °C, which showed there was no water present in the crystalline solid. Additionally, the experimentally determined $CO(NH_2)_2$ and SO_4^{2-} content in the solid DS* phase crystallized from their solid solutions showed 55.00% and 44.00% (wt), respectively, that was obtained from the elemental analysis of nitrogen and sulfur. This is in agreement with the stoichiometric values of 54.70% and 43.80% (wt). The data altogether confirmed that in the DS* regions $2CO(NH_2)_2 \cdot H_2SO_4$ crystallizes out of saturated solutions of varying composition.

Liquid Fertilizers from $2CO(NH_2)_2 \cdot H_2SO_4 - CO(NH_2)_2 - H_2O$ Ternary System. The $2CO(NH_2)_2 \cdot H_2SO_4 - CO(NH_2)_2 - H_2O$ ternary phase diagram in Figure 5 also shows the blue points corresponding to the concentrations obtained from the saturated solution curves that intersect 0 °C, shown in Figures 2 and 3. By definition, liquid fertilizer composition is defined in the saturated solutions that crystallize at 0 °C. In some instances, depending on the climate and liquid fertilizer use, liquid fertilizers that crystallize out of the saturated solutions at lower or higher temperatures than 0 °C can be used. Thus, the data in Figure 5 were used to formulate the compositions of the corresponding liquid N:S fertilizers based on $2CO(NH_2)_2 \cdot H_2SO_4$. The results are summarized in Table 3. It is shown that the maximum 27.38% nitrogen that can be obtained in the liquid fertilizers at 0 °C is made from the $2CO(NH_2)_2 \cdot H_2SO_4$ and $CO(NH_2)_2$ aqueous mixture. This corresponds to the 3.2:1 ratio of N:S. At the desired ratio of ~15:1 at 0 °C, 21.54% of nitrogen is observed. Increased temperatures afforded higher nitrogen content in liquid fertilizers with ~15:1 N:S content of 23.83% N at 10 °C. On the other hand, the lowest sulfur concentration was 0.96%, with the highest observed being 1.78% S at ~15:1 N:S ratio. The sulfur concentration in liquid fertilizers at 0 °C can vary anywhere from 0.87% to 11.21%. The composition of the liquid fertilizer with closest to the exact 15:1 N:S ratio crystallizes at 10 °C and has 14.76% N and 0.96% S. To prepare true liquid fertilizer that crystallizes at 0 °C, a solution containing 39.50% urea, 12.10% diurea sulfate, and 48.40% water needs to be used. Summertime liquid fertilizers can be made from the 45.00% urea, 11.10 diurea sulfate, and 44.00% water, containing 23.83%

Table 3. Physicochemical Properties of Proposed Liquid N- and S-Containing Fertilizers Based on Diurea Sulfate

| solution composition (wt %)									
U*	DS*	H$_2$O	N	S	nutrient ratio (N:S)	crystallization temperature (°C)	pH	dynamic viscosity (mPa s)	Density (kg/m^3)
~15:1 N:S ratio, various temperatures									
28.50	7.15	64.35	15.13	1.05	14.1:1	−10.0	1.30	1.774	1110
28.04	6.55	65.41	14.76	0.96	15.3:1	−10.0	1.32	1.770	1107
35.44	11.40	53.16	19.45	1.67	11.6:1	−7.5	1.35	2.089	1153
37.02	7.45	55.53	19.18	1.09	17.5:1	−5.0	1.50	1.944	1140
39.50	**12.10**	**48.40**	**21.54**	**1.78**	**12.1:1**	**0.0**	**1.40**	**2.434**	**1170**
45.00	11.00	44.00	23.83	1.61	14.8:1	10.0	1.56	2.641	1180
45.00	10.00	45.00	23.57	1.47	16.0:1	10.0	1.52	2.507	1176
various N:S ratios									
40.50	5.95	53.55	20.43	0.87	23.5:1	0.0	−	−	−
39.50	**12.10**	**48.40**	**21.54**	**1.78**	**12.1:1**	**0.0**	**1.40**	**2.434**	**1170**
38.50	18.45	43.05	22.70	2.71	8.4:1	0.0	−	−	−
37.20	25.12	37.68	23.81	3.69	6.5:1	0.0	−	−	−
35.00	32.50	32.50	24.68	4.77	5.2:1	0.0	−	−	−
33.45	39.93	26.62	25.87	5.86	4.4:1	0.0	−	−	−
31.10	48.23	20.67	26.90	7.08	3.8:1	0.0	−	−	−
21.50	62.80	15.70	26.16	9.22	2.8:1	0.0	−	−	−
26.15	59.08	14.77	27.38	8.67	3.2:1	0.0	−	−	−
2.36	76.40	21.24	20.73	11.21	1.8:1	0.0	−	−	−
5.00	75.00	20.00	21.60	11.01	2.0:1	0.0	−	−	−
8.25	72.50	19.25	22.48	10.64	2.1:1	0.0	−	−	−
11.70	70.75	17.55	23.63	10.39	2.3:1	0.0	−	−	−
16.10	67.80	16.10	24.93	9.95	2.5:1	0.0	−	−	−
36.25	27.50	36.25	23.97	4.04	5.9:1	0.0	−	−	−
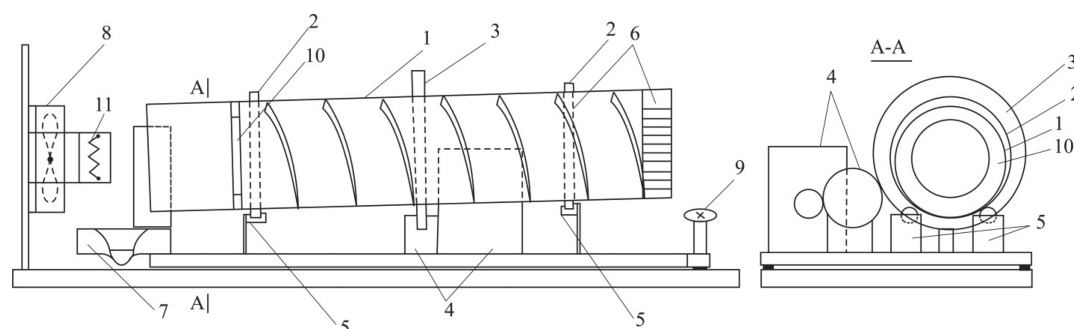
Figure 6. Side and end view schematics of the lab-scale rotary drum granulator dryer used in this work to obtain granulated diurea sulfate-based composite N−P−K fertilizers. It is comprised of (1) granulator drum, (2) supporting ring, (3) pinion, (4) electrical engine with the reduction drive, (5) support rollers, (6) material lifters, (7) granule discharge duct, (8) ventilator, (9) granulator inclination angle adjuster, (10) overflow ring, and (11) electrical heater.

N and 1.61% S with a N:S ratio of 14.8. It would crystallize at 10 °C.

Finally, the physical properties of the liquid fertilizers based on diurea sulfate with a N:S ratio of ∼15:1 shown in Table 3 were measured. The properties examined were pH, dynamic viscosity, and density. This information is critical in defining technological parameters during the process plant design. It is shown from Table 3 that solution density varies from 1107 to 1180 kg/m^3, whereas dynamic viscosity varies from 1.770 to 2.641 mPa s. The pH measured was very low, <2, showing that these fertilizers are mostly suitable for very alkaline soils.

Granulation of Diurea Sulfate Compound Fertilizers and Their Chemical and Physical Properties. As discussed previously, diurea sulfate inherits physical and chemical properties of its parent materials and thus is hygroscopic; it absorbs moisture at moderate relative humidities. This presents major difficulties during its storage due to the particle softening,

which increases its volume, reduces its granulate particle strength, and increases caking (tendency to form agglomerates). Additionally, diurea sulfate incorporates a strong acid (H$_2$SO$_4$) in its molecular unit that results in low pH values of <2 (Table 3). This effectively limits its applicability as a fertilizer to highly alkaline soils because high acidity results in decline of soil fertility and low productivity. A typically used procedure to remedy this is soil treatments using lime or other alkaline earth compounds, such as calcium or magnesium carbonates, hydroxides, and oxides.[43] A clearly attractive option is the granulation of diurea sulfate with alkaline fine material. The granulated product would result in reduced caking and slower nutrient distribution into the soil, and sulfuric acid could redistribute into other chemical compounds of lower acidity. Literature on the granulation of diurea sulfate is very scarce, and the authors of this work have not been able to find any reports. Urea sulfate has been used previously as a liquid binder

to improve solution–solid phase ratios and was generated via reaction between urea and sulfuric acid in the granule.[44] To our knowledge, this is the first attempt to use diurea sulfate in its solid form to obtain compound fertilizer granules. Finally, granulation is a convenient way of incorporating other nutrients, such as phosphorus, into the same granule,[45] which was also performed.

Granulation is a complex multivariable process with many input variables influencing multiple product properties. However, for particle nucleation, wetting is needed; the liquid binder is brought into contact with a dry powder bed and is distributed through the bed to give a distribution of nuclei granules.[46] Other granulation variables typically include a solid feed rate, fine powder feed rate, drum rotation rate, and drum inclination angle.[47] A lab-scale rotating drum granulator dryer that was built for this work, shown in Figure 6, allowed for altering of the above parameters. Only the granulator inclination angle was varied from 2° to 5°, whereas rotation speed was kept at 20 min⁻¹. Several granulation procedures were attempted. First, we granulated diurea sulfate crystals, obtained after their synthesis, using a variable ratio of using H_2O as a liquid binder while altering the diurea sulfate/H_2O ratio. We changed the moisture content from 2% to 7%, and in all cases, we observed growth of the crystal agglomerates. However, even when a minimum force was applied, these granules broke down into separated particles. It is known that granulation takes place due to capillary and cohesive–adhesive forces between the solid particles due to recrystallization of the base powder.[38] It can be proposed that crystalline bridges between the diurea sulfate particles do not form or form slower than the normal residence time of the granule within the granulator. This is consistent with the observations that very slow diurea sulfate crystallization occurs from its saturated solutions.[25] In the next step, the granulation procedure was altered to include a solid filler material, which is known to enhance granule physical properties.[48] A slurry containing 5%, 10%, 15%, 20%, 25%, 35%, and 50% (wt) dolomite with diurea sulfate was prepared and supplied into the granulator, whereas the granulator inclination angle was systematically adjusted from 3° to 5° and moisture content of the slurry was adjusted from 2% to 7%. The maximum value of moisture was governed by the ensuing solubility of diurea sulfate resulting in the cessation of the granulation process. Granulation onset was observed when 10% dolomite was present in the mixture supplied to the granulator. Moisture content was confined to 4%, and the inclination angle between 3° and 5° was sufficient to sustain the granulation process. A slight increase in the necessary moisture content was observed with an increasing dolomite amount with 15%, 20%, 25%, and 35% of dolomite in the mixture requiring between 5% and 7% of moisture to form and grow granules. The resulting granule crushing strength, however, was not satisfactory in all cases with the measured values ranging from 0.631 to 0.715 MPa for 15%, 20%, and 25% of dolomite with a maximum of 1.823 MPa obtained for 35% dolomite. Further increase in the dolomite content did not result in increased granule crushing strength. It must be noted that a typical desired crushing strength of the compound N–P–K fertilizer granules varies between 2 and 4 MPa, depending on client specifications.[35]

Next in the diurea sulfate granulation process, we attempted to use gypsum hemihydrate (also known as phosphogypsum), $CaSO_4 \cdot 0.5H_2O$, a byproduct of the wet phosphoric acid, H_3PO_4, production process. It is produced via an exothermic reaction (reaction 1) at 87–95 °C via a reaction between fluorapatite and H_2SO_4

$$4Ca_5(PO_4)_3F + 20H_2SO_4 + 10H_2O$$
$$\rightarrow 12H_3PO_4 + 20CaSO_4 \cdot 0.5H_2O + 4HF \tag{1}$$
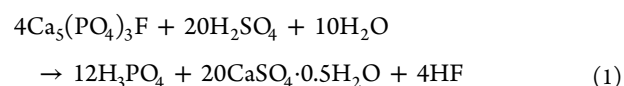
and accumulates in tremendous amounts as waste. Approximately, 30 million tons is produced annually in the United States alone, and up to 300 million tons is produced annually worldwide.[49,50] Its sustainable reuse is of tremendous importance[51] and could potentially serve as an alkaline calcium source to bind diurea sulfate into the granule. A slurry containing 5%, 10%, and 15% (wt) of phosphogypsum with diurea sulfate was prepared and supplied into the granulator, whereas the granulator inclination angle and moisture content were systematically adjusted. The granulated product was only obtained at 5° inclination and 3% moisture content. Granules were obtained, but their crushing strengths were measured at 0.837, 0.922, and 1.046 MPa for the respective phosphogypsum amounts, thus not resulting in acceptable physical granule properties. One proposed chemical process that would result in rather low physical strength granules can be proposed to proceed via a reaction of H_2SO_4 and carbonates ($MgCO_3$ + $CaCO_3$) in dolomite (reaction 2)

$$2CO(NH_2)_2 \cdot H_2SO_4 + MgCO_3 + CaCO_3$$
$$\rightarrow MgSO_4 + CaSO_4 + 2CO(NH_2)_2 + H_2O + CO_2 \tag{2}$$
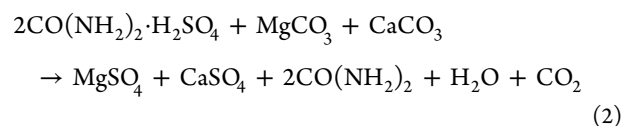
thus resulting in decomposition of dolomite. Finally, granulation of the compound fertilizers was explored using diurea sulfate with phosphorus- and potassium-containing minerals and dolomite as a filler. This is due to the increasing need in the compound nitrogen/phosphorus/potassium-containing fertilizers, where all three nutrients are contained within one granule. Additionally, a flexible composition range can be obtained within one granule, and it can be adjusted depending on the soil needs. To obtain compound N–P–K fertilizer granules using diurea sulfate, we chose potassium chloride, KCl, and diammonium phosphate, $(NH_4)_2HPO_4$, as the corresponding sources of potassium and phosphorus. Granules were obtained, albeit under very narrow experimental condition ranges. Specifically, the inclination angle of the granulator was 5°, and moisture content added was 7%. Additionally, only when the entrance temperature of the slurry material was 50 ± 1 °C and that of the exit temperature was 38 ± 1 °C were high quality granules obtained. This is due to the need to have elevated temperatures to recrystallize certain compound fertilizer components, which is necessary for bridge formation between the particles.
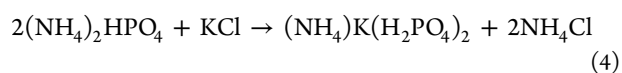
Stable N–P–K granules of 16–16–16–5.5(S)–0.4(MgO)–0.6(CaO) grade, obtained using these granulation parameters, were stored at room temperature (23 °C) and a relative humidity of 50%. The crushing strength of these granules was measured as a function of storage time, and the data obtained is shown in Table 4. The crushing strength of the 16–16–16–5.5(S)–0.4(MgO)–0.6(CaO) granules obtained using diurea sulfate, potassium chloride, diammonium phosphate, and dolomite as raw materials increased up to 30 days after the granulation from 2.370 to 3.159 to 3.800 MPa and remained constant afterward. Additionally, after 30 days of storage, the final product contained 15.90% nitrogen (9.20% urea and 6.70% ammoniacal), 16.00% P_2O_5, 16.10% K_2O, 5.50% sulfur,

Table 4. Crystalline Compounds Present in 16−16−16−5.5(S)−0.4(MgO)−0.6(CaO) Granulated Fertilizers after 10, 20, and 30 Day Curing, As Determined from Their XRD Patterns[a]

curing time after the granulation (days)	compounds detected	granule crushing strength (MPa)
10	$CO(NH_2)_2 \cdot H_3PO_4$, $((NH_4)_{0.30}K_{0.70})_2SO_4$, $K(NH_4)Ca(SO_4)_2 \cdot H_2O$, NH_4Cl, KCl, $CaSO_4$, $NH_4H_2PO_4$	2.730
20	$CO(NH_2)_2 \cdot H_3PO_4$, $((NH_4)_{0.30}K_{0.70})_2SO_4$, $K_{0.11}(NH_4)_{0.89}(H_2PO_4)$, $CO(NH_2)_2 \cdot NH_4Cl$, $NH_4H_2PO_4$	3.159
30	$CO(NH_2)_2 \cdot H_3PO_4$, $((NH_4)_{0.30}K_{0.70})_2SO_4$, $K_{0.11}(NH_4)_{0.89}(H_2PO_4)$, $CO(NH_2)_2 \cdot NH_4Cl$, $MgCO_3$, NH_4Cl, $CaMg(CO_3)_2$, KCl	3.800

[a]Experimentally obtained data were referenced against the corresponding International Center for Diffraction Data (ICDD) PDF-2 database XRD patterns: KCl (PDF #41-1476), CaSO₄ (PDF #26-328), NH₄Cl (PDF #7-7), NH₄H₂PO₄ (PDF #37-1479), K(NH₄)Ca-(SO₄)₂·H₂O (PDF #20-865), ((NH₄)₀.₃₀K₀.₇₀)₂SO₄ (PDF #83-2005), CO(NH₂)₂·H₃PO₄ (PDF #44-815), K₀.₁₁(NH₄)₀.₈₉(H₂PO₄) (PDF #82-2267), CO(NH₂)₂·NH₄Cl (PDF #44-722), MgCO₃ (PDF #8-479), and CaMg(CO₃)₂ (PDF #36-426).

0.40% MgO, and 0.60% CaO, showing that no loss of the nutrients happened. However, it is known that chemical reactions within the granule continue proceeding long after the granulation for up to 30 days (so-called product *curing*[52]). The products formed can significantly affect the long-term storage properties of the granules, such as caking. For example, the formation of ammonium chloride has been reported to be a major cause of the granule caking in compound fertilizer due to the ammonium chloride forming crystal bridges between the adjacent particles.[53] To determine the length of this period for these fertilizers, as well as the possible chemical reactions proceeding during the storage and the corresponding final products forming, we performed XRD analysis of the granules at 10, 20, and 30 days after the granulation. The chemical composition of the resulting compounds are shown in Table 4 with the corresponding XRD pattern peak assignments provided in Tables S1−S3 of the Supporting Information. These data were referenced against the corresponding International Center for Diffraction Data (ICDD) PDF-2 database XRD patterns: KCl (PDF #41-1476), CaSO₄ (PDF #26-328), NH₄Cl (PDF #7-7), NH₄H₂PO₄ (PDF #37-1479), K(NH₄)-Ca(SO₄)₂·H₂O (PDF #20-865), ((NH₄)₀.₃₀K₀.₇₀)₂SO₄ (PDF #83-2005), CO(NH₂)₂·H₃PO₄ (PDF #44-815), K₀.₁₁(NH₄)₀.₈₉(H₂PO₄) (PDF #82-2267), CO(NH₂)₂·NH₄Cl (PDF #44-722), MgCO₃ (PDF #8-479), and CaMg(CO₃)₂ (PDF #36-426). The results from the XRD study show that a complex chemical reaction network takes place within 30 days of storage. In particular, after 10 days of storage, XRD peaks due to NH₄H₂PO₄ can be observed with the corresponding interplanar spacings of 0.532, 0.376, 0.307, 0.265, 0.237, and 0.201 nm. Additionally, K(NH₄)Ca(SO₄)₂·H₂O is present with the corresponding interplanar spacings of 0.980, 0.358, 0.307, and 0.237 nm, as well as those due to NH₄Cl and KCl. The former can be formed via reactions 3 and 4

$$(NH_4)_2HPO_4 + 2KCl \rightarrow 2NH_4Cl + K_2HPO_4 \tag{3}$$

$$2(NH_4)_2HPO_4 + KCl \rightarrow (NH_4)K(H_2PO_4)_2 + 2NH_4Cl \tag{4}$$

and result in a stable crystalline compound with urea via reaction 5

$$CO(NH_2)_2 + NH_4Cl \rightarrow CO(NH_2)_2 \cdot NH_4Cl \tag{5}$$

.
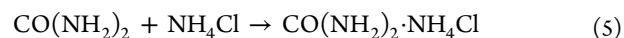
Additional crystalline phases detected after 10 days of storage were $CaSO_4$, $((NH_4)_{0.30}K_{0.70})_2SO_4$ and $CO(NH_2)_2 \cdot H_3PO_4$. $CaSO_4$ can possibly be formed via reaction 6

$$2CO(NH_2)_2 \cdot H_2SO_4 \cdot + CaCO_3$$
$$\rightarrow CaSO_4 + 2CO(NH_2)_2 + H_2O + CO_2 \tag{6}$$
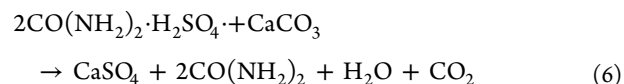
Interplanar spacing observed in this work for CaSO₄ at 0.437 nm, however, overlaps with that of CO(NH₂)₂·H₃PO₄, and thus, its presence cannot be unambiguously determined. XRD data obtained from the granules stored for 20 days showed the presence of two main compounds: CO(NH₂)₂·NH₄Cl and CO(NH₂)₂·H₃PO₄. Formation of the latter proceeds via reaction 7

$$2CO(NH_2)_2 \cdot H_2SO_4 + (NH_4)_2HPO_4$$
$$\rightarrow CO(NH_2)_2 + CO(NH_2)_2 \cdot H_3PO_4 + (NH_4)_2SO_4 \tag{7}$$
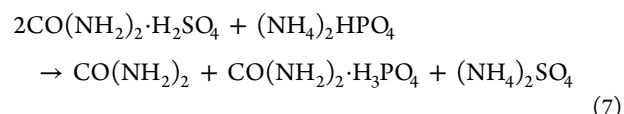
with an equimolar amount of (NH₄)₂SO₄ formed. Additional phases determined to be present were ((NH₄)₀.₃₀K₀.₇₀)₂SO₄ and K₀.₁₁(NH₄)₀.₈₉(H₂PO₄). No calcium or magnesium containing crystalline compounds were inferred from XRD patterns, possibly due to their low relative amount. Crystalline compounds detected after 30 days of granule storage were predominantly due to the CO(NH₂)₂·H₃PO₄, CO(NH₂)₂·NH₄Cl, and ((NH₄)₀.₃₀K₀.₇₀)₂SO₄. Minor amounts of KCl, NH₄Cl, and K₀.₁₁(NH₄)₀.₈₉(H₂PO₄) were also be detected. Overall, these data show that the 16−16−16−5.5(S)−0.4-(MgO)−0.6(CaO) granules obtained using diurea sulfate, potassium chloride, diammonium phosphate, and dolomite as raw materials change their chemical composition within 30 days of storage resulting in several intermediary and final compounds, including CO(NH₂)₂·H₃PO₄, CO(NH₂)₂·NH₄Cl, ((NH₄)₀.₃₀K₀.₇₀)₂SO₄, and K₀.₁₁(NH₄)₀.₈₉(H₂PO₄). These compounds dissolve in water very well and thus can be readily utilized by plants in soil. Calcium and magnesium appear to remain in the form of dolomite.

Conclusions and Broader Impact. Liquid and compound solid N−P−K fertilizers, containing both nitrogen and sulfur, were synthesized in this work. They are based on diurea sulfate, a high nitrogen- and sulfur-containing compound. We based our approach on the need of obtaining high nitrogen content fertilizers while eventually obtaining a 15:1 N:S nutrient ratio. For this purpose, we constructed ternary 2CO(NH₂)₂·H₂SO₄−CO(NH₂)₂−H₂O phase diagrams and synthesized fertilizers based on it. This approach is different from the CO(NH₂)₂−H₂SO₄−H₂O ternary system-based fertilizers proposed in earlier patents,[28−33] based on the early fundamental phase determination work by Dalman,[25] that show the maximum available nitrogen amount due to the use of diurea. Due to the low pH (<2) values of the resulting solution and known urea sulfate use as a binder material,[44] we used dolomite, in combination with phosphorus and potassium sources (diammonium sulfate and potassium chloride), to obtain 16−16−16−5.5(S)−0.4(MgO)−0.6(CaO) compound granulated fertilizers. A complex chemical reaction network and the resulting

2485

dx.doi.org/10.1021/sc500512b | ACS Sustainable Chem. Eng. 2014, 2, 2477−2487

products were monitored via XRD for up to 30 days of granulated product curing.

On a broader note, the elemental sulfur supply is projected to increase from 59.33 million (metric) tons in 2014 to 73.29 million tons in 2018, with 93% of the supply coming from oil and gas production facilities. This represents an approximate 3 million ton sulfur surplus annually in 2016−2018.[54] Sulfur production at petroleum refineries has increased in the past decades at a faster rate than the refineries have increased input due to the increasing sulfur content in oil. Effectively, there is no need to voluntarily produce sulfur using, for example, the Frasch method, but there is always an extra sulfur supply available to satisfy any increase in the demand. For example, Abu Dhabi is projected to process 1 billion cubic feet a day of sour gas into 500 million cubic feet of gas after removing sulfur from the supply in 2015. Habshan-5, an Abu Dhabi Gas Industries (GASCO) facility, was completed in 2013 to produce 5200 tons/day of sulfur as a byproduct of sour gas production. Currently, ∼90% of the sulfur is used for H_2SO_4 production thus accounting for ∼200 million tons of H_2SO_4 produced annually. Production of H_2SO_4 from elemental sulfur via contact process on either Pt or V_2O_5 catalysts is a very well-established technological process, the scale of which can always be expanded depending on the H_2SO_4 demand. About 50% of H_2SO_4 produced is used for fertilizer, mostly phosphate production, thus not reaching the soil as fertilizers but ending up stored in the gypsum form near the processing site.

Most of the current demand for the main N−S fertilizer, ammonium sulfate, is met by its production as a byproduct in various industries, such as nylon. The sulfur amount in soil, however, is projected to decrease due to the delicate combination of anthropogenic and natural processes that decrease emission of sulfur oxides, which in turn then do not result in atmospheric H_2SO_4 deposition in soil. However, sulfur is necessary to efficiently utilize nitrogen at a ratio of these nutrients of 15:1 (N:S).[5,7,8] Currently, the main input of sulfur to the soil from mineral fertilizers is via compound N−P−K fertilizers, to which sulfate has been added at 2−5% sulfur in the mineral form, e.g. as K_2SO_4, $MgSO_4$, and $(NH_4)_2SO_4$, thus decreasing the mass concentration of nitrogen. The former two need to be obtained by mining, thus not sustainably utilizing the excess refinery elemental sulfur. The method of making liquid and compound granulated N−P−K fertilizers, described in this work, effectively utilizes existing scalable H_2SO_4 production technologies to obtain these N−S-containing fertilizers. This avoids unsustainable use of sulfate minerals, while supplying necessary sulfur in the form of nitrogen-rich diurea sulfate. Furthermore, the described method of obtaining N−S fertilizers is not tied to the utilization of the other industry byproduct $(NH_4)_2SO_4$ and thus does not depend on the supply/demand of, for example, caprolactam production, but rather on the largest possible scale industry (oil and gas), thus avoiding any supply fluctuations.

■ ASSOCIATED CONTENT

Ⓢ Supporting Information

Summary of the granulated 16−16−16−5.5(S)−0.4(MgO)−0.6(CaO) fertilizer crystallographic analysis after 10, 20, and 30 days of storage. This material is available free of charge via the Internet at http://pubs.acs.org.

■ AUTHOR INFORMATION

Corresponding Author

*E-mail: job314@lehigh.edu. Phone +1-610-758-6836.

Notes

The authors declare no competing financial interest.

■ ACKNOWLEDGMENTS

■ REFERENCES

(1) Schroeder, J. I.; Delhaize, E.; Frommer, W. B.; Guerinot, M. Lou; Harrison, M. J.; Herrera-Estrella, L.; Horie, T.; Kochian, L. V.; Munns, R.; Nishizawa, N. K.; et al. Using membrane transporters to improve crops for sustainable food production. *Nature* **2013**, *497*, 60−66.

(2) Rockstrom, J.; Steffen, W.; Noone, K.; Persson, A.; Chapin, F. S.; Lambin, E. F.; Lenton, T. M.; Scheffer, M.; Folke, C.; Schellnhuber, H. J.; et al. A safe operating space for humanity. *Nature* **2009**, *461*, 472−475.

(3) Gelfand, I.; Sahajpal, R.; Zhang, X.; Izaurralde, R. C.; Gross, K. L.; Robertson, G. P. Sustainable bioenergy production from marginal lands in the US Midwest. *Nature* **2013**, *493*, 514−517.

(4) Foyer, C. H.; Noctor, G.; Buchanan, B.; Dietz, K.-J.; Pfannschmidt, T. Redox regulation in photosynthetic organisms: Signaling, acclimation, and practical implications. *Antioxid. Redox Signaling* **2009**, *11*, 861−905.

(5) Abdallah, M.; Dubousset, L.; Meuriot, F.; Etienne, P.; Avice, J.-C.; Ourry, A. Effect of mineral sulphur availability on nitrogen and sulphur uptake and remobilization during the vegetative growth of *Brassica napus* L. *J. Exp. Bot.* **2010**, *61*, 2635−2646.

(6) De Bona, F. D.; Fedoseyenko, D.; von Wirén, N.; Monteiro, F. A. Nitrogen utilization by sulfur-deficient barley plants depends on the nitrogen form. *Environ. Exp. Bot.* **2011**, *74*, 237−244.

(7) Fismes, J.; Vong, P. .; Guckert, A.; Frossard, E. Influence of sulfur on apparent N-use efficiency, yield and quality of oilseed rape (*Brassica napus* L.) grown on a calcareous soil. *Eur. J. Agron.* **2000**, *12*, 127−141.

(8) Jamal, A.; Moon, Y.-S.; Abdin, M. Z. Sulphur − A general overview and interaction with nitrogen. *Aust. J. Crop Sci.* **2010**, *4*, 523−529.

(9) Salvagiotti, F.; Ferraris, G.; Quiroga, A.; Barraco, M.; Vivas, H.; Prystupa, P.; Echeverría, H.; Gutiérrez Boem, F. H. Identifying sulfur deficient fields by using sulfur content; N:S ratio and nutrient stoichiometric relationships in soybean seeds. *Field Crops Res.* **2012**, *135*, 107−115.

(10) Juszczuk, I. M.; Ostaszewska, M. Respiratory activity, energy and redox status in sulphur-deficient bean plants. *Environ. Exp. Bot.* **2011**, *74*, 245−254.

(11) Edwards, A. C.; Coull, M.; Sinclair, A. H.; Walker, R. L.; Watson, C. A. Elemental status (Cu, Mo, Co, B, S and Zn) of Scottish agricultural soils compared with a soil-based risk assessment. *Soil Use Manage.* **2012**, *28*, 167−176.

(12) Grant, C. A.; Mahli, S. S.; Karamanos, R. E. Sulfur management for rapeseed. *Field Crops Res.* **2012**, *128*, 119−128.

(13) Hopkins, F. E.; Turner, S. M.; Nightingale, P. D.; Steinke, M.; Bakker, D.; Liss, P. S. Ocean acidification and marine trace gas emissions. *Proc. Natl. Acad. Sci. U.S.A.* **2010**, *107* (760−765), S760/1−S760/8.

(14) Bates, T. S.; Lamb, B. K.; Guenther, A.; Dignon, J.; Stoiber, R. E. Sulfur emissions to the atmosphere from natural sources. *J. Atmos. Chem.* **1992**, *14*, 315−337.

(15) Sunda, W.; Kieber, D. J.; Kiene, R. P.; Huntsman, S. An antioxidant function for DMSP and DMS in marine algae. *Nature* **2002**, *418*, 317−320.

(16) Six, K. D.; Kloster, S.; Ilyina, T.; Archer, S. D.; Zhang, K.; Maier-Reimer, E. Global warming amplified by reduced sulphur fluxes as a result of ocean acidification. *Nat. Clim. Change* **2013**, *3*, 975−978.

(17) Cofala, Z. K.; S, J. S.; J. The last decade of global anthropogenic sulfur dioxide: 2000−2011 emissions. *Environ. Res. Lett.* **2013**, *8*, 14003.

(18) Stanislaus, A.; Marafi, A.; Rana, M. S. Recent advances in the science and technology of ultra low sulfur diesel (ULSD) production. *Catal. Today* **2010**, *153*, 1−68.

(19) Ma, X.; Velu, S.; Kim, J. H.; Song, C. Deep desulfurization of gasoline by selective adsorption over solid adsorbents and impact of analytical methods on ppm-level sulfur quantification for fuel cell applications. *Appl. Catal. B* **2005**, *56*, 137−147.

(20) Chandra Srivastava, V. An evaluation of desulfurization technologies for sulfur removal from liquid fuels. *RSC Adv.* **2012**, *2*, 759−783.

(21) Chung, W. J.; Griebel, J. J.; Kim, E. T.; Yoon, H.; Simmonds, A. G.; Ji, H. J.; Dirlam, P. T.; Glass, R. S.; Wie, J. J.; Nguyen, N. A.; et al. The use of elemental sulfur as an alternative feedstock for polymeric materials. *Nat. Chem.* **2013**, *5*, 518−524.

(22) Honsel, A.; Kojima, M.; Haas, R.; Frank, W.; Sakakibara, H.; Herschbach, C.; Rennenberg, H. Sulphur limitation and early sulphur deficiency responses in poplar: significance of gene expression, metabolites, and plant hormones. *J. Exp. Bot.* **2012**, *63*, 1873−1893.

(23) Thomas, J. M.; Raja, R. Design of a "green" one-step catalytic production of ε-caprolactam (precursor of nylon-6). *Proc. Natl. Acad. Sci. U.S.A.* **2005**, *102*, 13732−13736.

(24) Chou, M.-I. M.; Bruinius, J. A.; Benig, V.; Chou, S.-F. J.; Carty, R. H. Producing ammonium sulfate from flue gas desulfurization by-products. *Energy Sources* **2005**, *27*, 1061−1071.

(25) Dalman, L. H. Ternary systems of urea and acids. I. Urea, nitric acid and water. II. Urea, sulfuric acid and water. III. Urea, oxalic acid and water. *J. Am. Chem. Soc.* **1934**, *56*, 549−553.

(26) Hicks, G. C.; Stinson, J. M. Pilot-plant production of urea-ammonium sulfate. *Ind. Eng. Chem. Process Des. Dev.* **1975**, *14*, 269−276.

(27) Chen, T.; Xiao, S.; Zhong, B.; Stern, C. L.; Ellis, D. E. Uronium sulfate, $[OHC(NH_2)_2]_2 (SO_4)$. *Acta Crystallogr. Sect. C* **1999**, *55*, 994−996.

(28) Young, D. C. *Noncorrosive Urea-Sulfuric Acid Compositions*. U.S. Patent US4402852 A, 1983.

(29) Young, D. C. *Methods of Producing Concentrated Urea-Sulfuric Acid Reaction Products*. U.S. Patent US4445925 A, 1984.

(30) Young, D. C. *Noncorrosive Urea-Sulfuric Acid Reaction Products*. U.S Patent 4404116 A, 1983.

(31) Young, D. C. *Method of Producing Urea-Sulfuric Acid Reaction Products*. U.S. Patent US4397675 A, 1983.

(32) Young, D. C. *Topical Fertilization Methods and Compositions for Use therein*. U.S. Patent US4447253 A, 1984.

(33) Harbolt, B. A.; Moerdyke, D. D. *Single Pass Continuous Urea-Sulfuric Acid Process*. U.S. Patent US4962283 A, 1990

(34) Koebel, M.; Strutz, E. O. Thermal and hydrolytic decomposition of urea for automotive selective catalytic reduction systems: Thermochemical and practical aspects. *Ind. Eng. Chem. Res.* **2003**, *42*, 2093−2100.

(35) *Regulation (EC) No. 2003/2003 of the European Parliament and of the Council of 13 October 2003 Relating to Fertilisers*; Official Journal of the European Union. L 304-1, 2003.

(36) Macrae, C. F.; Edgington, P. R.; McCabe, P.; Pidcock, E.; Shields, G. P.; Taylor, R.; Towler, M.; van de Streek, J. Mercury: Visualization and analysis of crystal structures. *J. Appl. Crystallogr.* **2006**, *39*, 453−457.

(37) Rutland, D. W. *Manual for Determining Physical Properties of Fertilizer*; The International Fertilizer Development Center: Muscle Shoals, AL, 1986; p 91.

(38) Salman, A. D.; Hounslow, M. J.; Seville, J. P. K.; Eds.; *Granulation: Handbook of Powder Technology*; Elsevier B.V.: Oxford, U.K., 2007.

(39) Egal, M.; Budtova, T.; Navard, P. The dissolution of microcrystalline cellulose in sodium hydroxide-urea aqueous solutions. *Cellulose* **2008**, *15*, 361−370.

(40) Fang, H. L.; DaCosta, H. F. M. Urea thermolysis and NOx reduction with and without SCR catalysts. *Appl. Catal. B* **2003**, *46*, 17−34.

(41) Lundström, A.; Andersson, B.; Olsson, L. Urea thermolysis studied under flow reactor conditions using DSC and FT-IR. *Chem. Eng. J.* **2009**, *150*, 544−550.

(42) Schaber, P. M.; Colson, J.; Higgins, S.; Thielen, D.; Anspach, B.; Brauer, J. Thermal decomposition (pyrolysis) of urea in an open reaction vessel. *Thermochim. Acta* **2004**, *424*, 131−142.

(43) Edmeades, D. C.; Ridley, A. M. Using Lime To Ameliorate Topsoil and Subsoil Acidity. In *Handbook of Soil Acidity*; Rengel, Z., Ed.; Marcel Dekker, Inc.: New York, 2003; pp 297−336.

(44) Xue, B. C.; Hao, Q.; Liu, T.; Liu, E. B. Effect of process parameters and agglomeration mechanisms on NPK compound fertiliser. *Powder Technol.* **2013**, *247*, 8−13.

(45) Chien, S. H.; Prochnow, L. I.; Cantarella, H. Recent developments of fertilizer production and use to improve nutrient efficiency and minimize environmental impacts. *Adv. Agron.* **2009**, *102*, 267−322.

(46) Iveson, S. M.; Litster, J. D.; Hapgood, K.; Ennis, B. J. Nucleation, growth and breakage phenomena in agitated wet granulation processes: A review. *Powder Technol.* **2001**, *117*, 3−39.

(47) Ronen, D.; Sanders, C. F. W.; Tan, H. S.; Mort, P. R.; Doyle, F. J. Predictive dynamic modeling of key process variables in granulation processes using partial least squares approach. *Ind. Eng. Chem. Res.* **2011**, *50*, 1419−1426.

(48) Slinksiene, R.; Baliutavicius, V. Influence of some granulation parameters on properties of NPK fertilizers. *Chem. Technol. (Kaunas, Lith.)* **2012**, 31−39.

(49) Smadi, M. M.; Haddad, R. H.; Akour, A. M. Potential use of phosphogypsum in concrete. *Cem. Concr. Res.* **1999**, *29*, 1419−1425.

(50) Hunter, A. H. *Use of Phosphogypsum Fortified with Other Selected Essential Elements as Soil Amendment on Low Cation Exchange Soils*; Publication 01-034-081; Florida Institute of Phosphate Research: Bartow, FL, 1989.

(51) Jianxi, L.; Su, Y.; Liping, M. Feasibility analysis for decomposition of phosphogypsum in cement precalciner. *Environ. Prog. Sustainable Energy* **2011**, *30*, 44−49.

(52) Cekinski, E.; Thomassin, J. H. Influence of calcium sulfate crystal size on the curing time of single superphosphate. *Nutr. Cycling Agroecosyst.* **1996**, *46*, 23−28.

(53) Walker, G. M.; Magee, T. R. A.; Holland, C. R.; Ahmad, M. N.; Fox, J. N.; Moffatt, N. A.; Kells, A. G. Caking processes in granular NPK fertilizer. *Ind. Eng. Chem. Res.* **1998**, *37*, 435−438.

(54) Heffer, P.; Prud'homme, M. *Fertilizer Outlook 2014−2018*. In 82nd IFA Annual Conference; International Fertilizer Industry Association (IFA): Sydney, Australia, 2014.